A tetraphenylethene-based highly emissive metallacage as a component of theranostic supramolecular nanoparticles

A Submission to the Proceedings of the National Academy of Science USA

PHYSICAL SCIENCES: Chemistry

Guocan Yu,[a] Timothy R. Cook,[d] Yang Li,[c] Xuzhou Yan,[b] Dan Wu,[c] Li Shao,[a] Jie Shen,[c] Guping Tang,[c] Feihe Huang,[a,1] Xiaoyuan Chen[e,1] and Peter J. Stang[b,1]

[a]State Key Laboratory of Chemical Engineering, Center for Chemistry of High-Performance & Novel Materials, Department of Chemistry, Zhejiang University, Hangzhou 310027. P. R. China.
[b]Department of Chemistry, University of Utah, 315 South 1400 East, Room 2020, Salt Lake City, Utah 84112, United States.
[c]Department of Chemistry, Institute of Chemical Biology and Pharmaceutical Chemistry, Zhejiang University, Hangzhou 310027, P. R. China.
[d]Department of Chemistry, University at Buffalo, State University of New York, 359 Natural Sciences Complex, Buffalo, New York 14260, United States.
[e]Laboratory of Molecular Imaging and Nanomedicine, National Institute of Biomedical Imaging and Bioengineering, National Institutes of Health, Bethesda, Maryland 20892, United States.
[1]To whom correspondence should be addressed. Email address: fhuang@zju.edu.cn; shawn.chen@nih.gov; stang@chem.utah.edu

Table of Contents (26 Pages)

Section A. Materials/General Methods/Instrumentation

Tetrakis(triphenylphosphine)palladium(0), methyl 4-boronobenzoate and other reagents were commercially available and used as received. Solvents were either employed as purchased or dried according to procedures described in the literature. Tetra-(4-bromophenyl)ethylene was synthesized by McMurry coupling of 1,4-bromophenone according to a reported method,[S1] the Suzuki coupling reaction between tetra(4-bromophenyl)ethylene and methyl 4-boronobenzoate afforded donor **3**.[S2] Compound **5** was synthesized according to a reported method.[S3] ^{1}H NMR and ^{13}C NMR spectra were recorded on a Bruker Avance DMX-500 spectrometer or on a Bruker Avance Ⅲ-400 spectrometry with internal standard TMS. DOSY spectra were collected on a Bruker Avance DMX-500 spectrometer with internal standard TMS. ^{31}P{^{1}H} NMR chemical shifts are referenced to an external unlocked sample of 85% H_3PO_4. UV-vis spectra were taken on a Shimadzu UV-3150 spectrophotometer. Mass spectra were recorded on a Micromass Quattro II triplequadrupole mass spectrometer using electrospray ionization and analyzed with the MassLynx software suite or a Bruker Esquire 3000 plus mass spectrometer (Bruker-Franzen Analytik GmbH, Bremen, Germany) equipped with an ESI interface and an ion trap analyzer. High-resolution mass spectrometry experiments were performed with a Bruker 7-Tesla FT-ICR mass spectrometer equipped with an electrospray source (Billerica, MA, USA). The melting points were collected on a SHPSIC WRS-2 automatic melting point apparatus. Scanning electron microscopy (SEM) investigations were carried out on a Multimode 8 instrument operating at an energy of 15 Kev or 20 Kev. Transmission electron microscopy (TEM) investigations were carried out on a HT-7700 instrument. The fluorescence experiments were conducted on a RF-5301 spectrofluorophotometer (Shimadzu Corporation, Japan). Dynamic light scattering (DLS) measurements were carried out using a 200 mW polarized laser source Nd:YAG (λ = 532 nm). The polarized scattered light was collected at 90 °in a self-beating mode with a Hamamatsu R942/02 photomultiplier. The signals were sent to a Malvern 4700 submicrometer particle analyzer system.

Fabrication of the Metallacage. *Cis*-Pt$(PEt_3)_2(OTf)_2$ (9.79 mg, 13.4 mM), **1** (4.91 mg, 6.72 mM) and **3** (2.15 mg, 3.36 mM) were placed in a 2-dram vial, followed by addition of D_2O (0.2 mL) and acetone-d_6 (0.8 mL). After 3 h of heating at 75 ℃, all solvent was removed by N_2 flow and then dried under vacuum. Acetone-d_6 (0.7 mL) was then added into each mixture. A clear solution was obtained after an additional 5 h of heating at 75 ℃. The metallacage was precipitated with diethyl ether, isolated and dried under reduced pressure. This precipitation-redissolve procedure was repeated three times, and then the metallacage was dissolved in CD_2Cl_2 for characterization. Herein, *cis*-$(PEt_3)_2Pt(OTf)_2$ was chosen as one of the building blocks because of its excellent anticancer ability. On the other hand, *cis*-$(PEt_3)_2Pt(OTf)_2$ has been widely utilized to fabricate metallacages and metallacycles. In our studies, we found that the cytotoxicity of OTf anions was relatively low. Moreover, the OTf anions might exchange with other anions in the PBS. So, we used the metallacage **4** directly without anion exchange.

Preparation of MNPs. The nanoparticles containing the metallacages were prepared *via* matrix-encapsulation method. Briefly, 1 mL of acetone solution containing **mPEG-DSPE** (25.0 mg), **Biotin-PEG-DSPE** (5.00 mg) and **4** (4.00 mg) was injected into 20 mL of MilliQ water, followed by sonication of the mixture for 90 s at 18 W output.

The mixture was then stirred at 600 rpm at room temperature in dark for 72 h for the evaporation of acetone. After passing through a 0.2 μm syringe filter, the **MNPs** suspension was obtained and stored at room temperature for further use.

The additional PEG groups provide increased biocompatibility for the metallacages safely housed within the hydrophobic core of the **MNPs**. In our system, the PEG segments on the shell of **MNPs** can form "brushlike" superstructures, which prevent proteins from penetrating the surface and circumvents secondary adsorption onto the outer surface of the PEG layer. This feature may help prolong circulation times and prevent the premature release of **4**, minimizing toxicity to normal tissue.

The method for the fabrication of the metallacage-loaded nanoparticles without biotin groups was similar to the preparation of **MNPs**. The nanoparticles containing the metallacages were prepared *via* matrix-encapsulation method. Briefly, 1 mL of acetone solution containing **mPEG-DSPE** (30.0 mg) and **4** (4.00 mg) was injected into 20 mL of MilliQ water, followed by sonication of the mixture for 90 s at 18 W output. The mixture was then stirred at 600 rpm at room temperature in dark for 72 h for the evaporation of acetone. After passing through a 0.2 μm syringe filter, the resultant suspension was obtained and stored at room temperature for further use.

Transmission Electron Microscopy (TEM) and Dynamic Light Scattering (DLS) Studies. The morphology of the nanoparticles was revealed using TEM. TEM samples were prepared by drop-coating the solution containing **mPEG-DSPE**, **Biotin-PEG-DSPE** and **4** onto a carbon-coated copper grid. The solution was left to stand about 12 h and the insoluble precipitate was eliminated by using a microporous membrane before being used for DLS tests. The stability of the nanoparticles was confirmed by measuring the mean diameters of nanoparticles after different periods of incubation by DLS tests.

Determination of Platinum Content in the Nucleus and Cytoplasm. Nuclei of the cells were collected following an established procedure.[S4] Briefly, the cells were seeded two days before treatment at a concentration of 4×10^5 cells/mL in 75 cm^2 cell culture flasks till 80 % of confluence. The cells were treated with **MNPs** (the concentration of Pt was 10.0 μM) for 6 h, the pellet collected after trypsinazation and washed 3 times with ice cold PBS. The pellet was incubated with lysis buffer (10 mM HEPES, 10 mM KCl, 1.5 mM $MgCl_2$, 0.5 mM dithiothreitol) to which protease cocktail was added for 10 minutes. Samples were homogenized in a 7 mL Dounce Homogenizator with a tight pestle. The suspension was centrifuged at 500 g for 5 minutes (4 ℃) and the supernatant was removed. The pellet was re-dissolved in 3 mL of a sucrose solution (0.25 M sucrose, 10 mM $MgCl_2$) and layered with 3 mL of a second hypertonic sucrose solution (0.35 M sucrose, 0.5 mM $MgCl_2$). The suspension was centrifuged at 1450 g for 5 minutes (4 ℃). The pellet was re-suspended in 3 mL of the second sucrose solution and centrifuged at 1450 g for 5 minutes (4 ℃) to obtain the pure nuclear extract. The supernatant phases discarded during the isolation procedure were collected and formed the rest fraction. An aliquot of crude lysate supernatant, nuclear fraction and rest (lysates without nuclei) was each used for protein quantification. The Pt content was determined by using ICP-MS.

Cell Culture. HeLa, HepG2, CHO and HEK293 cells were purchased from the American Type Culture Collection (ATCC, Rockville MD) and cultured in Dulbecco's modified Eagle's medium (DMEM) containing 10% fetal bovine serum (FBS) and 1% penicillin/streptomycin. Cells grew as a monolayer and were detached upon confluence using trypsin (0.5% *w*/*v* in phosphate-buffered saline). The cells were harvested from cell culture medium by incubating in the trypsin solution for 5 min. The cells were centrifuged, and the supernatant was discarded. A 3.00 mL portion of serum-supplemented DMEM was added to neutralize any residual trypsin. The cells were resuspended in serum-supplemented DMEM at a concentration of 1.00×10^4 cells/mL. Cells were cultured at 37 ℃ and 5% CO_2.

Cytotoxicity Evaluation. The cytotoxicity of **1**, **2**, **3** and **MNPs** against HeLa, HepG2, CHO and HEK293 cells were determined by 3-(4,5-dimethylthiazol-2-yl)-2,5-diphenyl tetrazolium bromide (MTT) assay in a 96-well cell culture plate. All solutions were sterilized by filtration with a 0.22 μm filter before tests. The cells were seeded at a density of 1.00×10^4 cells/well in a 96-well plate, and incubated for 24 h for attachment. Cells were then incubated with fresh serum-supplemented DMEM without/with **1**, **2**, **3** and **MNPs** at various concentrations for 24 h. Then 20 μL of a MTT solution (5.00 mg/mL) were added to each well. After 4 h of incubation at 37 ℃, the MTT solution was removed, and the insoluble formazan crystals that formed were dissolved in 100 μL of dimethylsulfoxide. The absorbance of the formazan product was measured at 570 nm using a spectrophotometer (Bio-Rad Model 680). Untreated cells in media were used as a control. To confirm internalization *via* biotin receptor-mediated endocytosis, a competition assay was performed that involved adding an excess of biotin into the culture media. HeLa and HepG2 cells were seeded into 96-well plates and pretreated with 100 μM of biotin. The culture media were refreshed after 2 h and treated with the **MNPs** and analyzed by MTT assay. All experiments were carried out with five replicates.

***In Vitro* Cell Accumulation of the MNPs Determined by Flow Cytometry.** Quantitative analysis of the cellular uptake of the **MNPs** was measured by flow cytometry. HeLa, HepG2, CHO and HEK293 cells were seeded at a density of 3.00×10^5 cells/well in 12-well cell culture plates. The cells were left to grow for 24 h in DMEM media containing 10% FBS at 37 °C in 5% CO_2 atmosphere. After 24 h, **MNPs** (the concentration of the metallacage was kept at 2.00 μM) were added into the wells and the cells were incubated for 0.5 h, 1 h, 2 h, and 4 h, respectively. Following incubation, cells were rinsed twice with PBS to remove residual **MNPs**. Cells were harvested by trypsinization and resuspended in 500 μL of phosphate-buffered saline (PBS) for flow cytometry analysis using the FACS Calibur flow cytometer (BD Facsealibur). Data shown are the mean fluorescent signal for 1.00×10^4 cells. Cells that were not treated with the **MNPs** were used as a control. Data was analyzed using the FlowJo software. To confirm internalization *via* biotin receptor-mediated endocytosis, a competition assay was performed that involved adding an excess of biotin into the culture media. HeLa and HepG2 cells were seeded into 12-well plates and pretreated with 100 μM biotin. The culture media were refreshed after 2 h and treated with the **MNPs** for 4 h and analyzed by flow cytometry.

***In Vitro* Cell Accumulation of the MNPs Determined by Confocal Laser Scanning Microscopy (CLSM).** HeLa, HepG2, CHO and HEK293 cells were treated with the **MNPs** (the concentration of the metallacage was kept at 2 μM) in the culture medium at 37 ℃ for 30 min, 2 h, and 4 h, respectively. The cells were washed three times with PBS and fixed with fresh 4.0% formaldehyde at room temperature for 15 min. After washing with PBS, the cells were stained with DAPI (1 μg/mL) for 15 min. The images were taken using a LSM-510 confocal laser scanning microscope (Zeiss, Germany) (100 × oil objective, 405/488 nm excitation). To confirm internalization *via* biotin receptor-mediated endocytosis, a competition assay was performed that involved adding an excess of biotin into the culture media. HeLa and HepG2 cells were seeded into 12-well plates and pretreated with 100 μM biotin. The culture media were refreshed after 2 h and treated with the **MNPs** for 4 h and analyzed by CLSM.

DNA Viscosity Experiments. Viscosity measurements were carried out to confirm the non-intercalative nature of **2** or **4**.[S7] ct-DNA (200 μM) was treated with varying concentrations of **2** or **4** in PBS at pH = 7.2. The average flow times of each sample (*t*) [corrected by average flow time of buffer alone (t_0) and recorded in triplicate] were calculated using Schott AVS 310 automated viscometer. The relative viscosities (η) were obtained from the average flow time values using the equation: $\eta = (t\text{-}t_0)/t_0$. The data was presented as a plot of relative specific viscosity $[(\eta/\eta_0)^{1/3}]$ *vs.* [Pt]/[DNA], where η and η_0 are the viscosities of DNA in the presence and absence of **2** or the matallacage.

Analyses of Cellular Uptake of the Platinum Content by ICP-MS. HeLa, HepG2, CHO and HEK293 cells were seeded at a density of 2.00×10^5 cells/well in 12-well cell culture plates. The cells were left to grow for 24 h in DMEM media containing 10% FBS at 37 °C in 5% CO_2 atmosphere. After 24 h, **MNPs** (the concentration of Pt was kept at 10 μM) were added into the wells and the cells were incubated for 1 h, 2 h, 3 h, and 4 h, respectively. Following incubation, the cells were washed, digested and collected, and the Pt content in cells was determined by inductively coupled plasma mass spectrometer (ICP-MS, Thermo Fisher Scientific). To confirm internalization *via* biotin receptor-mediated endocytosis, a competition assay was performed that involved adding an excess of biotin into the culture media. HeLa and HepG2 cells were seeded into 12-well plates and pretreated with 100 μM biotin. The culture media were refreshed after 2 h and treated with the **MNPs** for 0.5 h, 1 h, 2 h, and 4 h, respectively, and the Pt content in cells was determined by ICP-MS. All experiments were carried out with three replicates.

Determination of the Percentage of Apoptotic Cells at Different Stages by Annexin-V FITC/PI Assay. 5×10^5 cells for each cell line (HeLa, HepG2) were seeded into six-well tissue culture plates and incubated overnight under standard growth conditions. The media for the cell lines were then replaced by fresh growth media with and without **2** with a Pt content of 4.0 μM. Treatment groups for each cell line were replicated three times. Cells were then incubated for 48 h at 37 ℃ and harvested with 0.25% trypsin. Cells were washed with PBS and subsequently stained by annexin-V FITC and propidium iodide (PI) in accordance with the manufacturer's protocol. Flow cytometrywas performed on the FACS Calibur flow cytometer (BD Facsealibur) and data were analyzed using BD FACSDiva. Untreated cells in media were used as a control.

Tumor Model. Female BALB/c nude mice (4 weeks old, ~20 g body weight) were purchased from Zhejiang Academy of Medical Sciences and maintained in a pathogen-free environment under controlled temperature (24 ℃). Animal care and handing procedures were in agreement with the guidelines evaluated and approved by the ethics committee of Zhejiang University. Study protocols involving animals were approved by the Zhejiang University Animal Care and Use Committee. The female nude mice were injected subcutaneously in the right flank region with 200 μL of cell suspension containing 5×10^6 HeLa cells. The tumors were allowed to grow to ~100 mm^3 before experimentation. The tumor volume was calculated as (tumor length) × (tumor width)^2/2. Relative tumor volumes were calculated as V/V_0 (V_0 was the tumor volume when the treatment was initiated).

p*K*s and Tissue Distributions. Mice received cisplatin, carboplatin, oxaliplatin or **MNPs** at a dose of 2 mg of Pt per kg body weight by tail vein injection. Animals were killed (three per time point) at 15 min, 1 h, 2 h, 4 h, 8 h, 12 h, 18 h, and 24 h after dosing. Blood was collected by cardiac puncture and kept in heparinized tubes. The amount of platinum in the plasma was determined by ICP-MS. The liver, lung, spleen, kidney and tumor were excised after *i.v*. injection of oxaliplatin, carboplatin, cisplatin or **MNPs** for 12 h and 24 h and kept in dry ice before analysis. Organs were digested in concentrated nitric acid for at least 24 h and the amount of platinum was analyzed by ICP-MS.

***In Vivo* Fluorescence Imaging.** When the tumor size reached around 100 mm^3, mice were *i.v*. injected with NPs fabricated from **3** or **MNPs**. Whole-body imaging was performed under the IVIS Kinetic Imaging System (Caliper Life Sciences, Hopkiton, MA) with excitation filter of 430 nm and emission filter of 620 nm before and after injection. All imaging parameters were kept constant for the whole imaging study.

***In Vivo* Antitumor Activity.** Tumor volume and body weights were measured for individual animals in all experiments. Tumor volume was determined by measuring the tumor in two dimensions with calipers and calculated using the formula tumor volume = (length × width^2)/2. The mice were divided into five treatment groups randomly (n = 10), when the mean tumor volume reached about 100 mm^3 and this day was set as day 0. Mice were administered intravenously with PBS, oxaliplatin, carboplatin, cisplatin or **MNPs** at dose of 2 mg Pt per kg body weight every 3 days for four times. Tumor volume and body weight were measured every 3 days. The tumor inhibition study was stopped on the 24th day.

Tissue Histopathology Evaluation. In the histological assay, the heart, liver, spleen, lung, kidney and tumor tissues were fixed in 4% paraformaldehyde for 24 h. The specimens were dehydrated in graded ethanol, embedded in paraffin, and cut into 5 mm thick sections. The fixed sections were deparaffinized and hydrated according to a standard protocol and stained with hematoxylin and eosin (H&E) for microscopic observation. Apoptosis of the tumor cells in the mice after treatments was determined by the TUNEL method according to the manufacturer's instructions. For analysis of cell proliferation, sections were incubated with anti-Ki67 antibody (1:25, ab28364, Abcam, United Kingdom), and then incubated with the secondary antibody of a Rb IgG (H+L)/HRP (ZB-2301, ZSGB-BIO, China) according to the manufacturer's instructions.

Section B. Synthesis and Characterization of the Highly Emissive Matallacage

*1. Synthesis of **1***

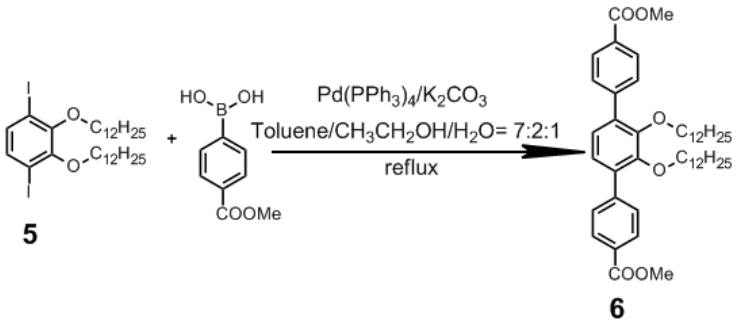

Synthesis of **6**: Methyl 4-boronobenzoate (1.44 g, 8.0 mmol), $Pd(PPh_3)_4$ (120 mg, 0.100 mmol) and K_2CO_3 (1.38 g, 10.0 mmol) were added to a solution of 1,4-diiodo-2,3-di(*n*-dodecyloxy)benzene (**5**) (1.40 g, 2.00 mmol) in the mixture of toluene, CH_3CH_2OH and H_2O (toluene/CH_3CH_2OH/H_2O = 7:2:1, *v*/*v*, 200 mL). The mixture was heated under nitrogen atmosphere at reflux for 48 h. The solvent was removed, and the residue was dissolved in dichloromethane and washed with water (5 × 50 mL). The organic layer was dried over anhydrous Na_2SO_4 and evaporated to afford the crude product, which was purified by flash chromatography using dichloromethane/methanol (10:1, *v*/*v*) as the fluent to afford **6** as a light yellow solid (1.80 g, 85%). mp 116.8−119.1 ℃. The proton NMR spectrum of **6** is shown in Figure S1. ^{1}H NMR (400 MHz, chloroform-*d*, room temperature) δ (ppm): 8.09 (d, J = 4.0 Hz, 4H), 7.66 (d, J = 4.0 Hz, 4H), 7.17 (s, 2H), 3.95 (s, 6H), 3.79 (t, J = 4.0 Hz, 4H), 1.52−1.48 (m, 4H), 1.31−1.16 (m, 36H), 0.88 (t, J = 8.0 Hz, 6H). The ^{13}C NMR spectrum of **6** is shown in Figure S2. ^{13}C NMR (100 MHz, chloroform-*d*, room temperature) δ (ppm): 169.70, 153.30, 145.56, 138.18, 132.05, 131.95, 131.42, 127.92, 76.53, 54.74, 34.57, 32.78, 32.32, 32.29, 32.26, 32.23, 32.01, 32.00, 28.59, 25.34, 16.76. LRESIMS is shown in Figure S3: *m*/*z* 736.1 $[M + Na]^+$ (100%). HRESIMS: *m*/*z* calcd for $[M + H]^+$ $C_{46}H_{67}O_6$, 715.4932, found 715.4944, error 1.7 ppm.

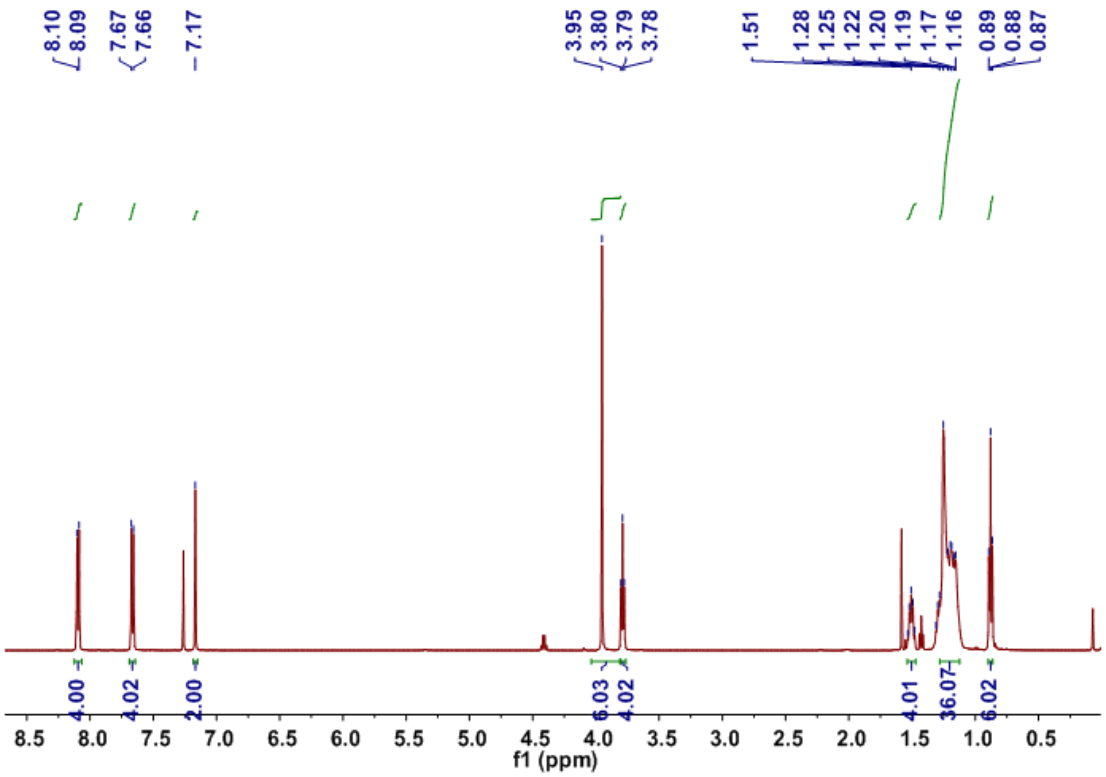

Figure S1. ^{1}H NMR spectrum (400 MHz, chloroform-*d*, room temperature) of **6**.

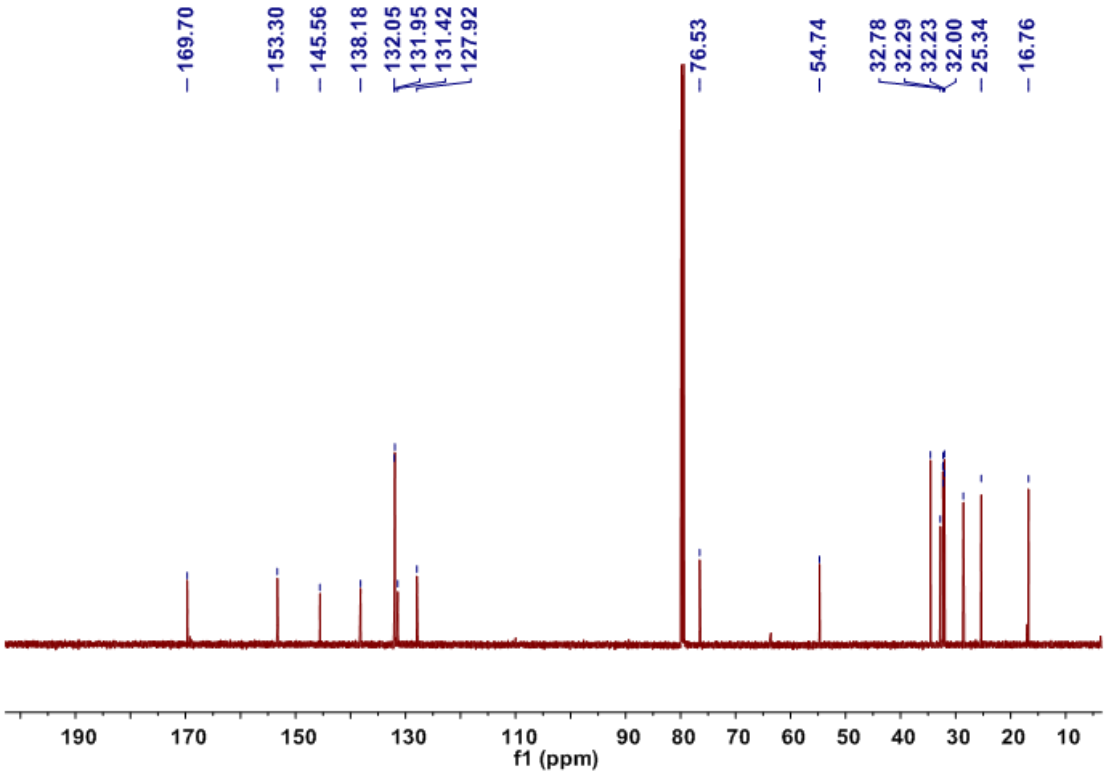

Figure S2. ^{13}C NMR spectrum (100 MHz, chloroform-*d*, room temperature) of **6**.

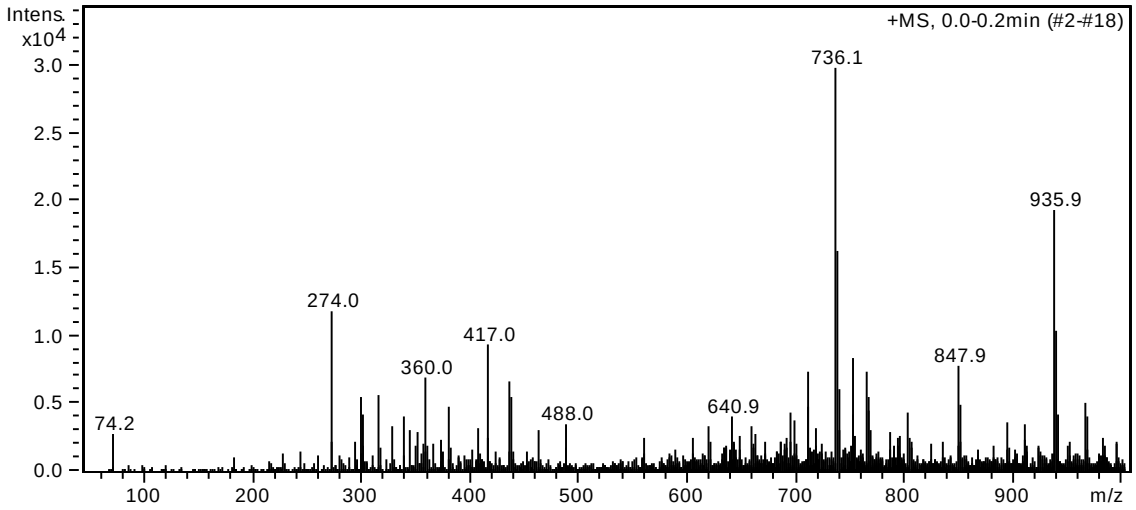

Figure S3. Electrospray ionization mass spectrum of **6**. Assignment of the main peak: *m*/*z* 736.1 $[M + Na]^+$ (100%).

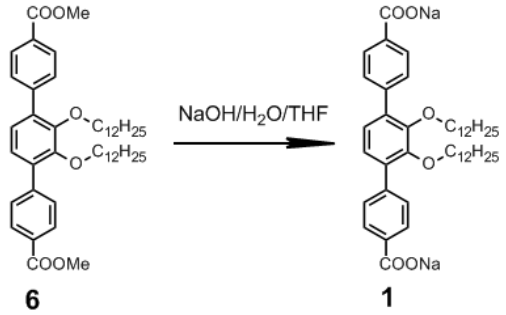

6 **1**

Synthesis of **1**: A solution of **6** (714 mg, 1.00 mmol) in THF (40 mL) was treated with 40% aqueous sodium hydroxide (40 mL) at reflux for 12 h. The mixture was concentrated under reduced pressure, and diluted with water (10 mL). The precipitate was collected by filtration, washed with water, and dried under vacuum to give **1** (642 mg, 88%) as a white solid, m.p. 127.5−129.8 ℃. The proton NMR spectrum of **1** is shown in Figure S4. ^{1}H NMR (400 MHz, acetone-d_6, room temperature) δ (ppm): 8.04 (d, J = 8.0 Hz, 4H), 7.69 (d, J = 8.0 Hz, 4H), 7.25 (s, 2H), 3.79 (t, J = 4.0 Hz, 4H), 1.50−1.45 (m, 4H), 1.24−1.14 (m, 36H), 0.86 (t, J = 8.0 Hz, 6H). The ^{13}C NMR spectrum of **1** is shown in Figure S5. ^{13}C NMR (100 MHz, chloroform-*d*, room temperature) δ (ppm): 167.09, 150.84, 149.67, 145.73, 140.13, 134.45, 125.15, 124.11, 77.22, 74.15, 31.93, 30.14, 29.68, 29.66, 29.62, 29.56, 29.37, 25.96, 22.70, 14.12. LRESIMS is shown in Figure S6: *m*/*z* 342.0 $[M - 2Na]^{2-}$ (100%), 685.0 $[M - 2Na + H]^-$ (53%). HRESIMS: *m*/*z* calcd for $[M - 2Na]^{2-}$ $C_{44}H_{60}O_6$, 342.4724, found 342.4732, error 2.3 ppm.

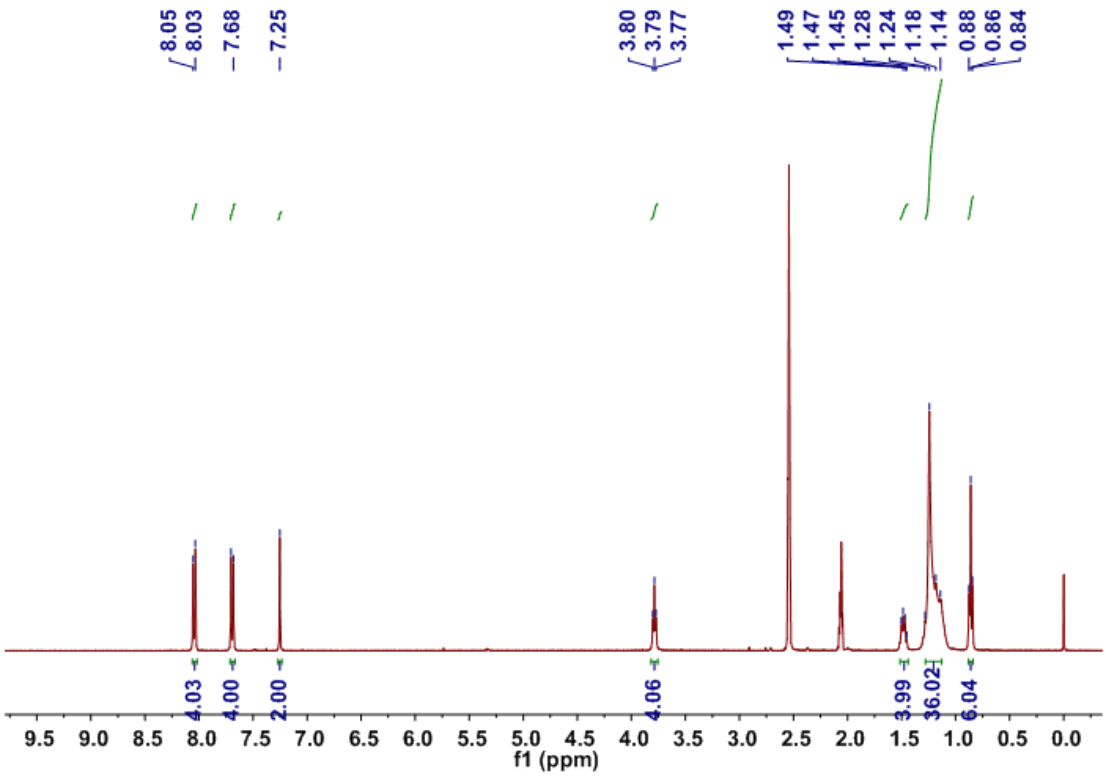

Figure S4. ^{1}H NMR spectrum (400 MHz, acetone-d_6, room temperature) of **1**.

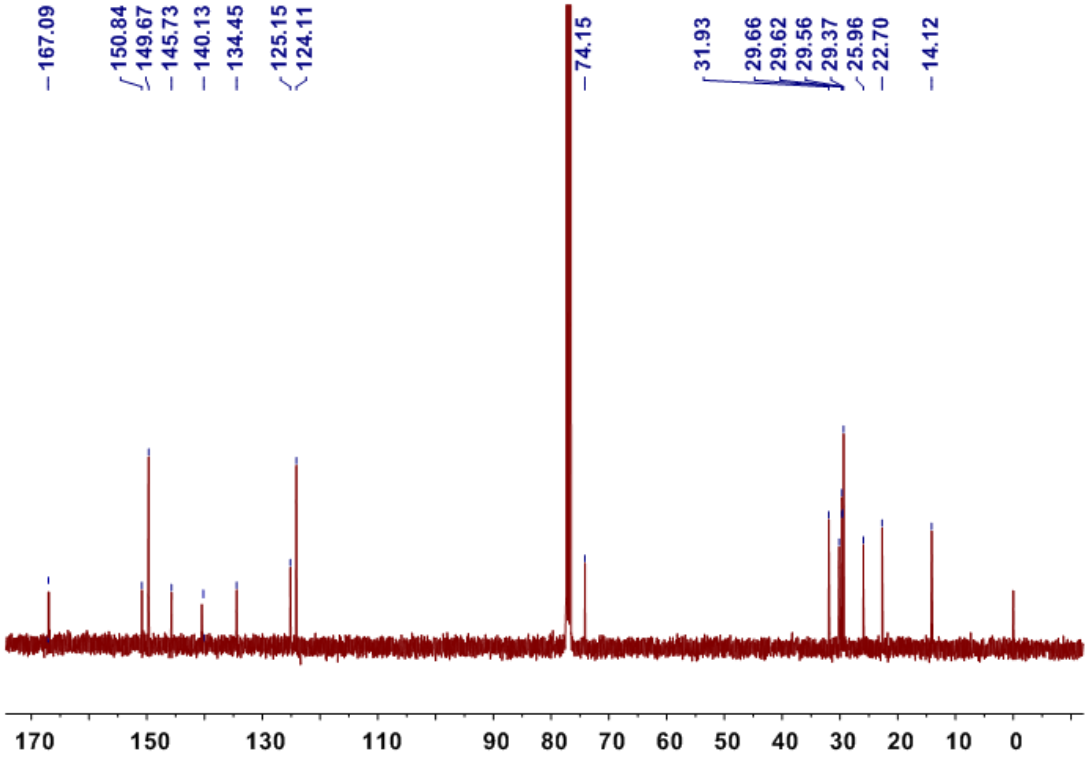

Figure S5. ^{13}C NMR spectrum (100 MHz, chloroform-*d*, room temperature) of **1**.

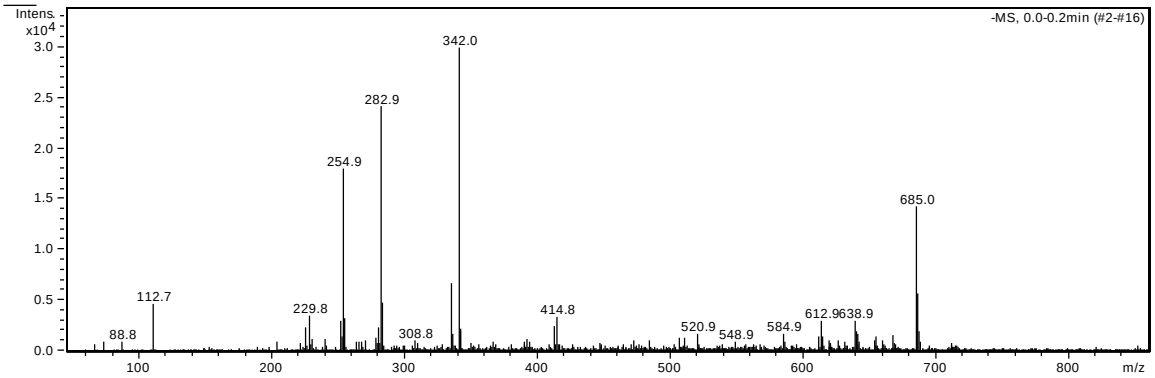

Figure S6. Electrospray ionization mass spectrum of **1**. Assignment of the main peak: *m*/*z* 342.0 $[M - 2Na]^{2-}$ (100%), 685.0 $[M - 2Na + H]^{-}$ (53%).

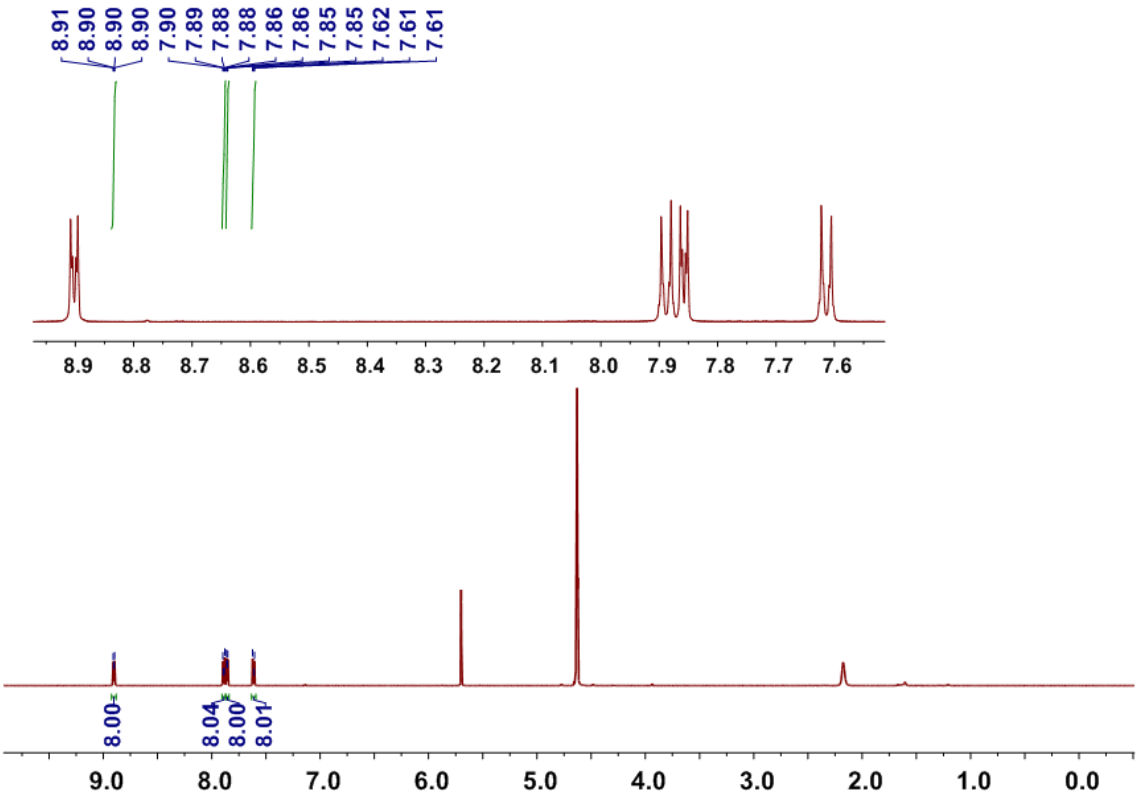

Figure S7. ^{1}H NMR spectrum (500 MHz, CD_2Cl_2/CD_3NO_2 = 2:1, room temperature) of **3**.

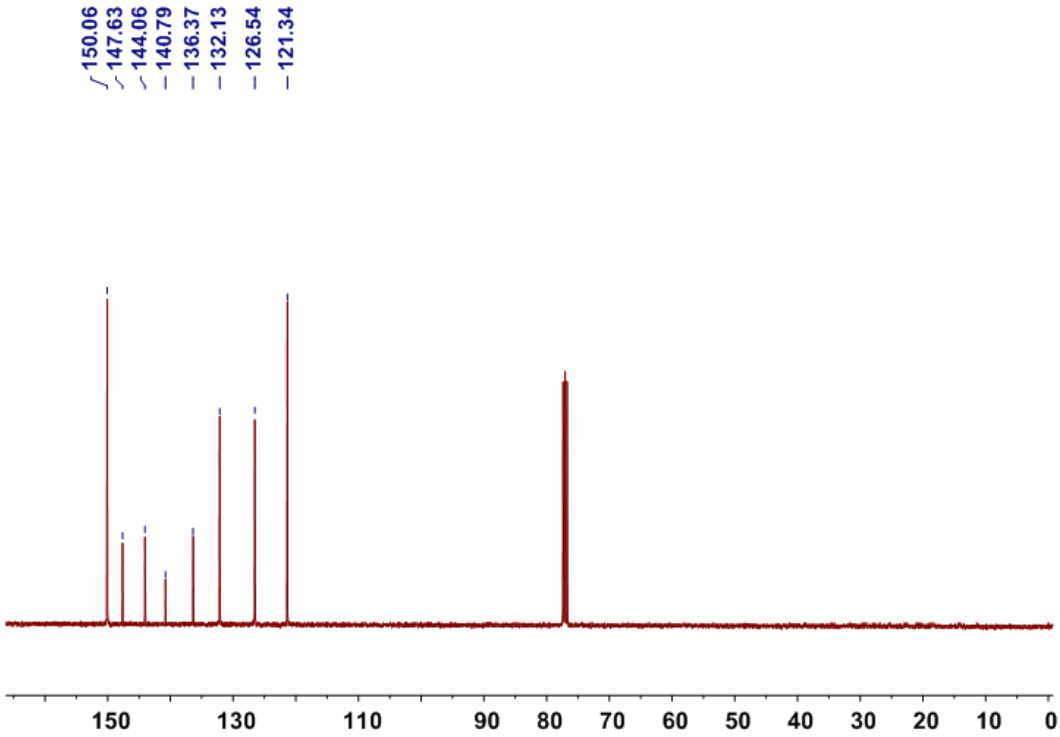

Figure S8. ^{13}C NMR spectrum (125 MHz, chloroform-*d*, room temperature) of **3**.

*2. Investigations on the formation of **4***

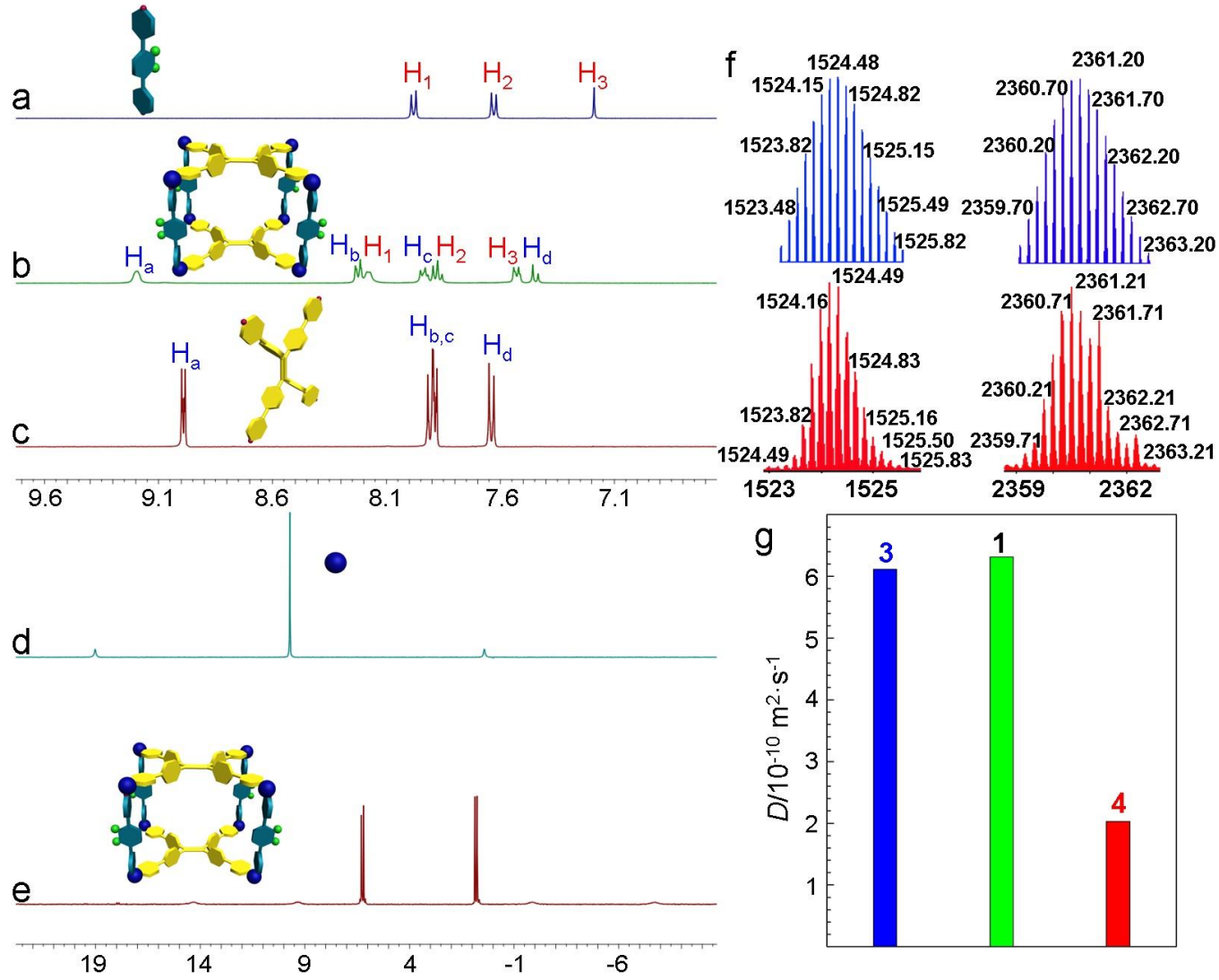

Figure S9. Partial ^{1}H NMR spectra (500 MHz, CD_2Cl_2, 293K) of (a) **1**, (b) **4**, and (c) **3**. $^{31}P\{^{1}H\}$ spectra (202.3 MHz, CD_2Cl_2, 293K) of (d) **2** and (e) **4**. (f) Experimental (red) and calculated (blue) electrospray ionization peaks of the $[M - 6OTf]^{6+}$ (left) and $[M - 4OTf]^{4+}$ (right) charge states of **4**. (g) Diffusion coefficient *D* values (CD_2Cl_2, 293K) of **1**, **3** and **4**.

3. Coordination-triggered aggregation-induced emission enhancement

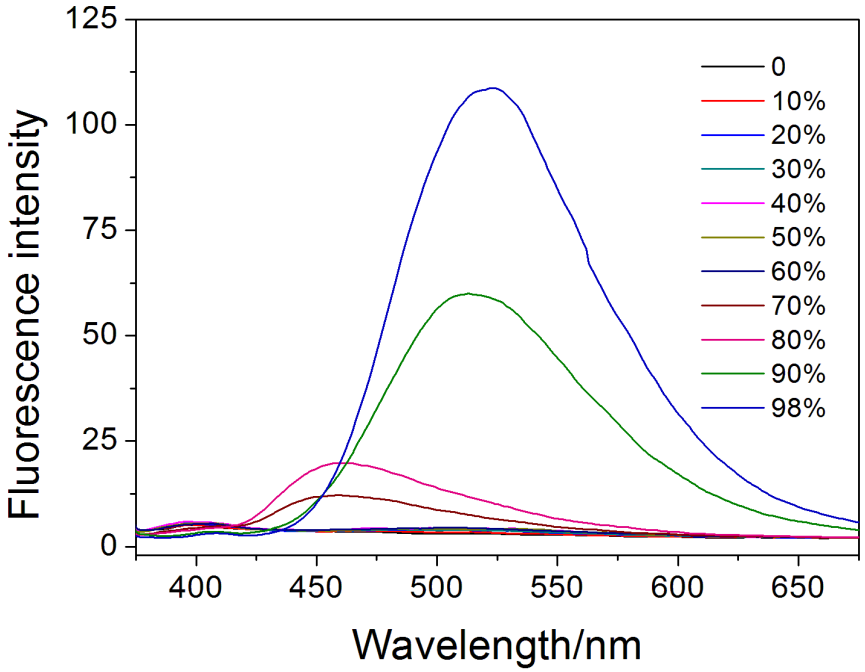

Figure S10. Fluorescence spectra of **3** in acetone and acetone/water mixtures. The concentration of the TPE group is 5.00 μM.

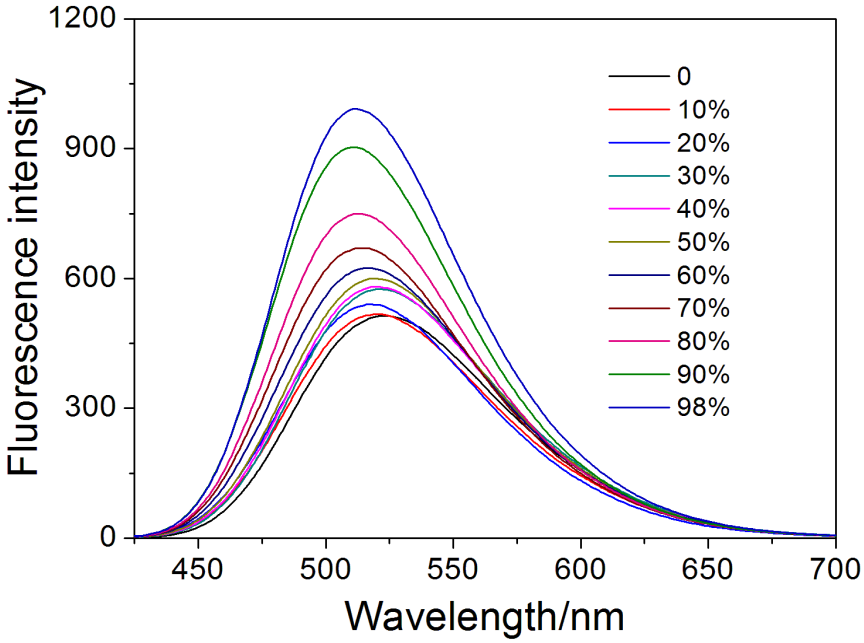

Figure S11. Fluorescence spectra of **4** in acetone and acetone/water mixtures. The concentration of the TPE group is 5.00 μM. It should be noted that the emission maximum of **4** in the mixtures of acetone and water changed with different f_w values.[S6]

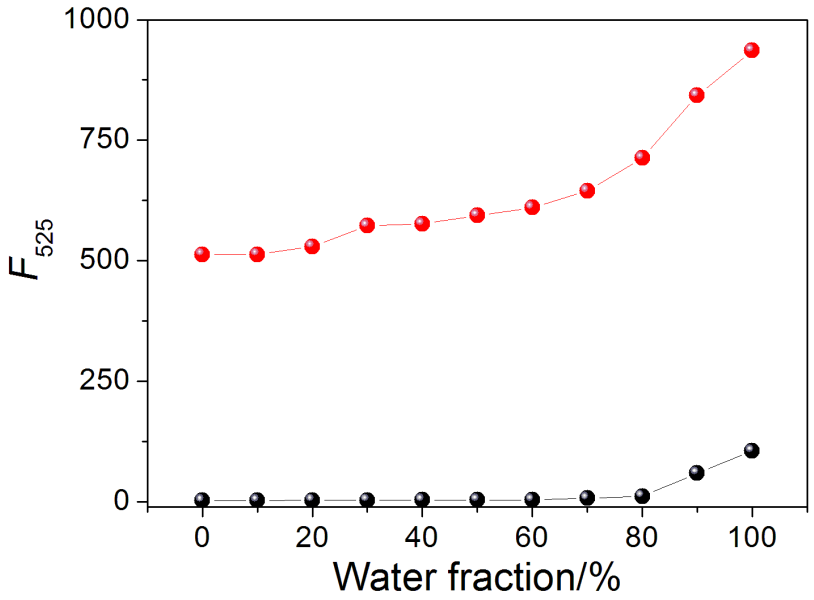

Figure S12. Plots of the emission intensities at 525 nm (F_{525}) *versus* water fractions (f_w) for **3** (●) and **4** (●) in acetone/water mixtures. The concentration of the TPE group is 5.00 μM.

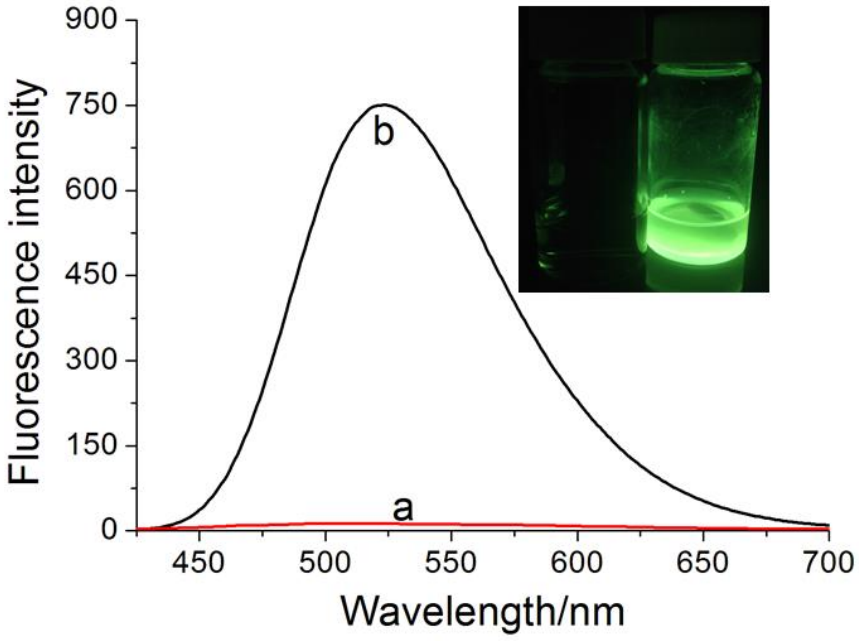

Figure S13. Fluorescence emission spectra of (a) **3** and (b) **4** in acetone.

3 is relatively weakly emissive in solution, while **4** is intensely emissive at ~525 nm at equivalent TPE concentration. The emission of **4** is attributed to the restricted rotation of the aromatic rings of the TPE groups upon coordination to the Pt nodes, thus preserving the AIE phenomenon in solution, in stark contrast to traditional AIE-based fluorogens.[S6]

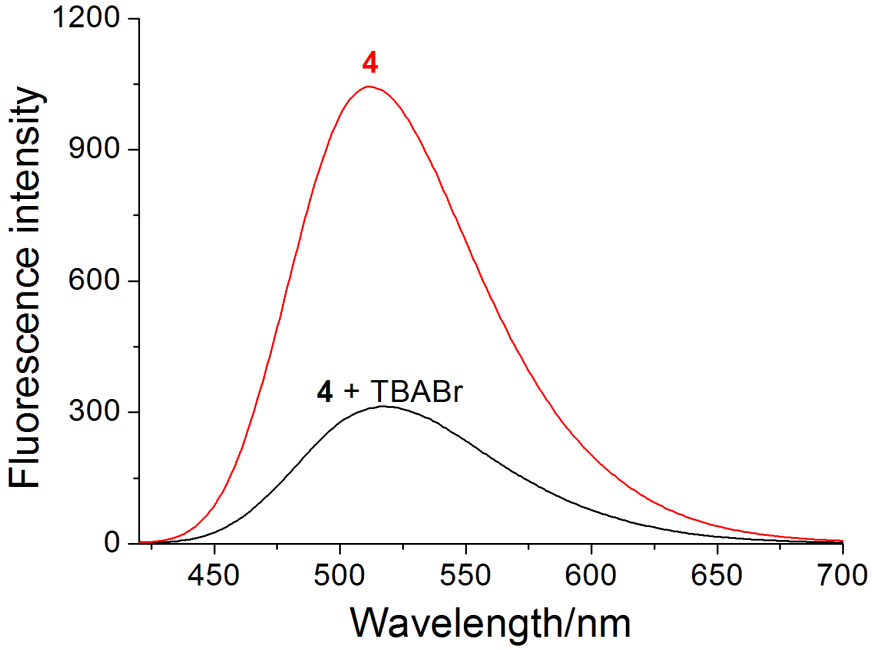

Figure S14. Fluorescence emission spectra of **4** in the absence and presence of TBABr in water.

Section C. Fabrication of MNPs and Theranostic Investigations

*1. Investigations on the formation of the **MNPs***

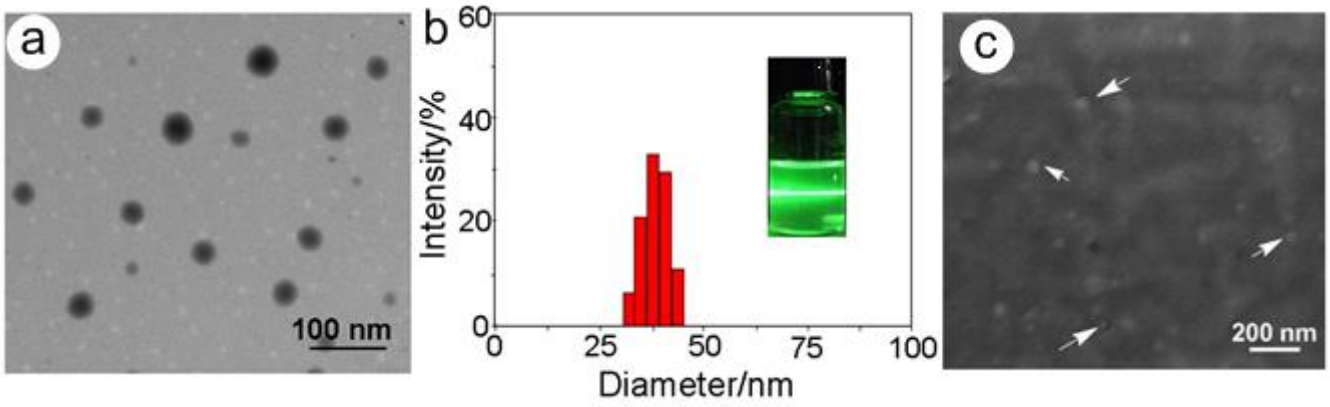

Figure S15. TEM image (a) and DLS result (b) of the **MNPs**. The inset photo is to show the Tyndall effect of an aqueous solution containing the **MNPs**. (c) SEM image of the **MNPs**.

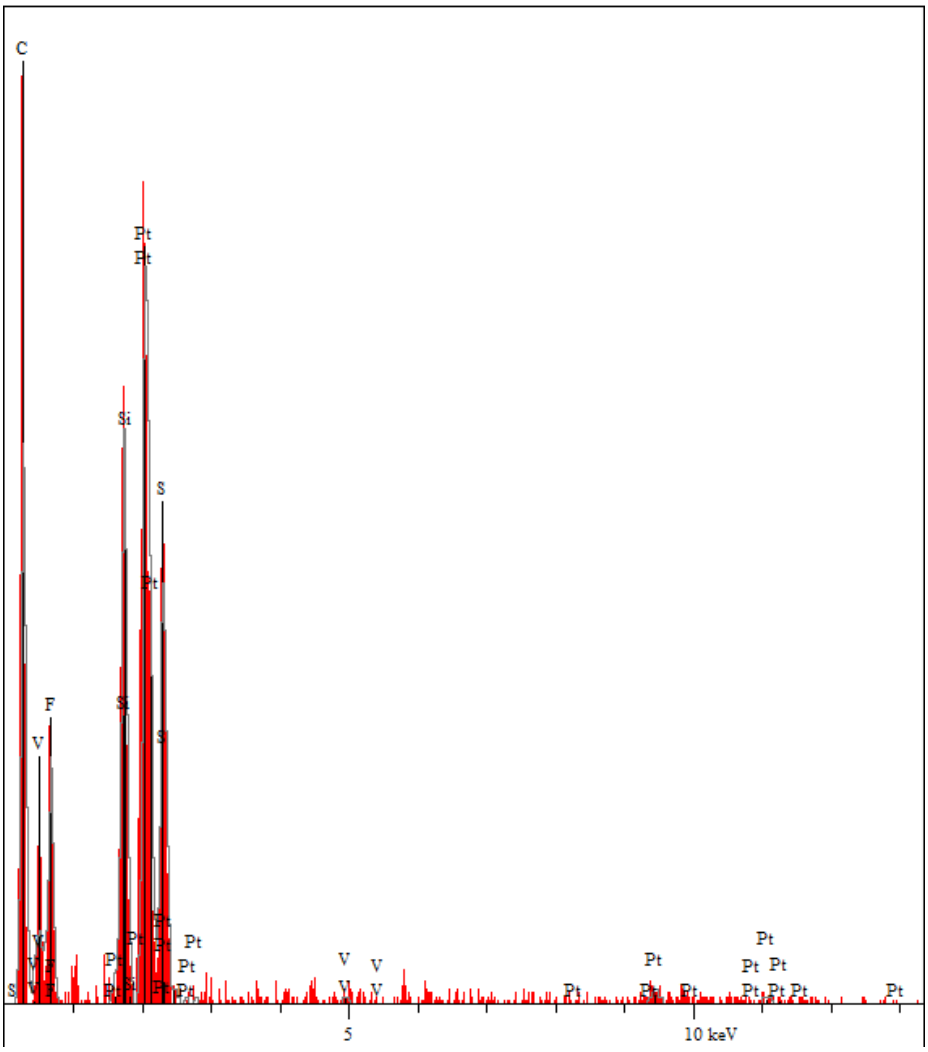

Figure S16. EDS study of the **MNPs**. EDS result demonstrated the existence of Pt in the **MNPs**, confirming that the metallacage **4** was encapsulated by the amphiphilic polymers (**mPEG-DSPE** and **Biotin-PEG-DSPE**).

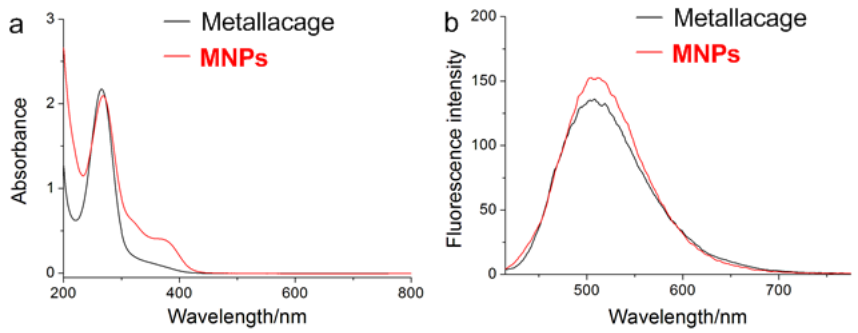

Figure S17. (a) UV-vis absorption and (b) fluorescence spectra of the metallacage and the **MNPs**.

From UV/Vis absorbance and fluorescent emission spectra, we knew that the features of **4** were almost unchanged upon formation of the **MNPs**, indicating that the encapsulation of the metallacages had a negligible effect on their photophysical properties.

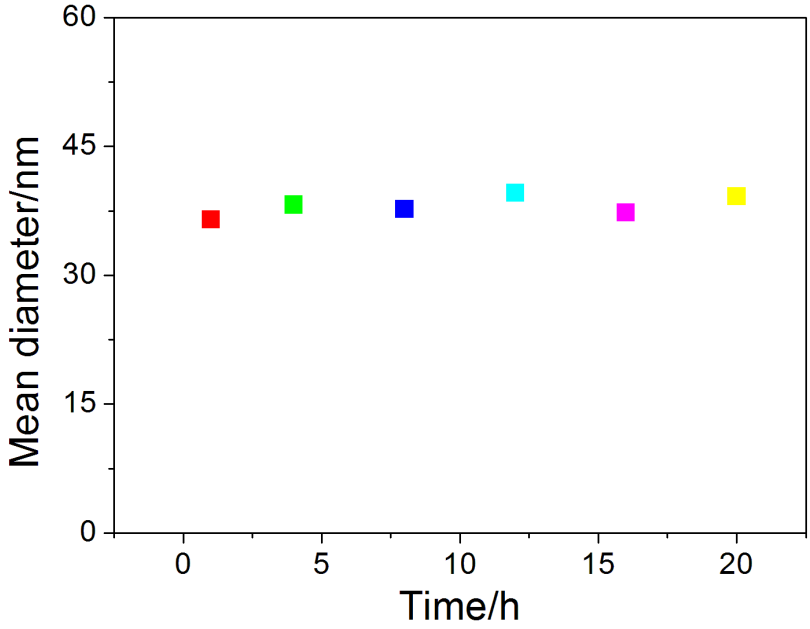

Figure S18. The average diameters of **MNPs** determined by DLS tests in PBS containing 10% FBS after different time periods of incubation.

In vitro release of Pt from the **MNPs** was studied using a dialysis bag diffusion method. In brief, 10 mg of **MNPs** in 2 mL of PBS (pH 7.4) was injected into a pre-swelled dialysis bag with a molecular weight cutoff of 1.0 kDa, followed by immersion into 18 mL of PBS at different solution pH values. The dialysis was conducted at 37 ^{o}C in a shaking culture incubator. Periodically, a 1 mL aliquot of sample solution from the incubation medium was taken for the measurement and compensated with 1 mL of fresh buffer into incubation medium. The concentration of platinum in the released solutions was quantified by ICP-MS measurement. The Pt released from the **MNPs** was expressed as the percentage of cumulative Pt outside the dialysis bag to the total Pt in the **MNPs**.

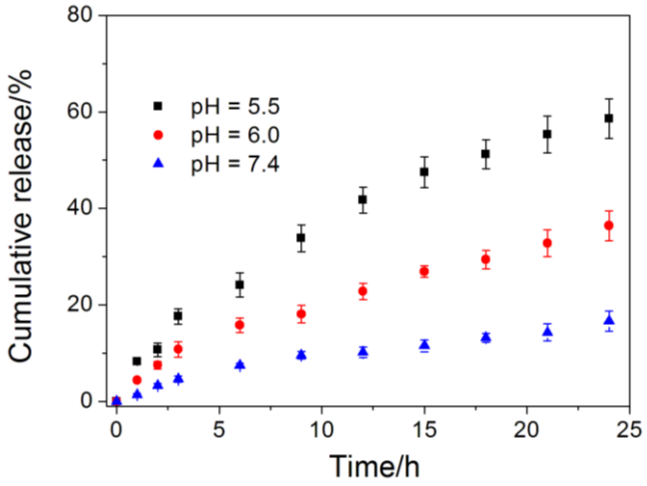

Figure S19. Release profiles of Pt from **MNPs** at different pH values.

The nanoparticles formed from **3** was prepared through a reprecipitation technique. Briefly, 1 mL of acetone solution containing **mPEG-DSPE** (25.0 mg), **Biotin-PEG-DSPE** (5.00 mg) and **3** (1.00 mg) was injected into 20 mL of MilliQ water, followed by sonication of the mixture for 90 s at 18 W output. The mixture was then stirred at

600 rpm at room temperature in dark for 72 h for the evaporation of acetone. After passing through a 0.2 μm syringe filter, the **NPs** suspension was obtained and stored at room temperature for further use.

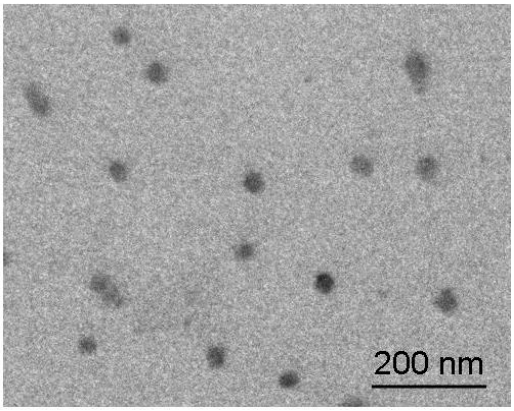

Figure S20. TEM image of the nanoparticles formed from **3**.

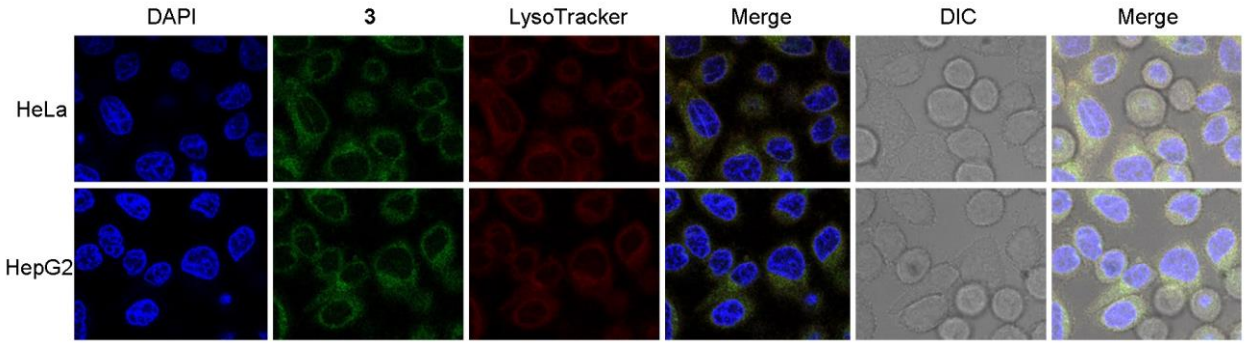

Figure S21. Confocal microscopy images of HeLa and HepG2 cells incubated with the NPs containing **3** for 4 h. The concentration of **3** was kept at 4 μM.

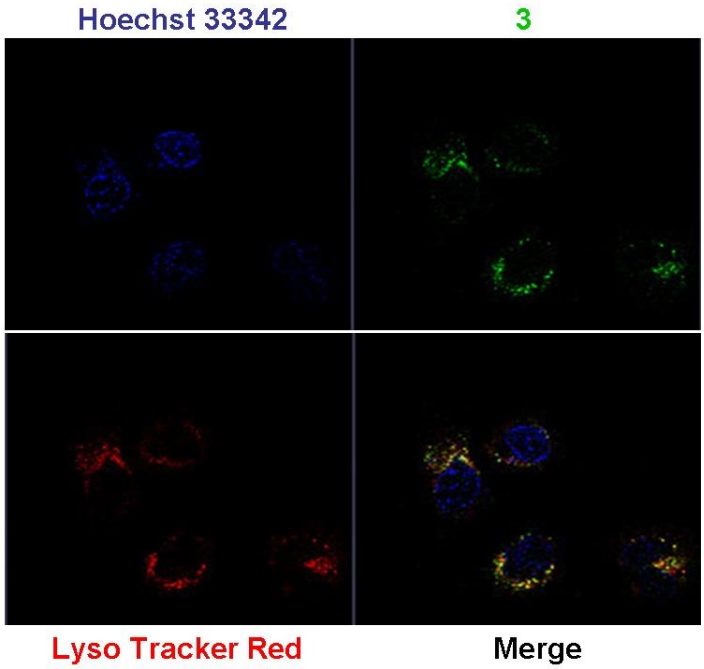

Figure S22. Confocal microscopy images of living HeLa cells incubated with the NPs formed from **3** for 4 h. The concentration of **3** was 4 μM.

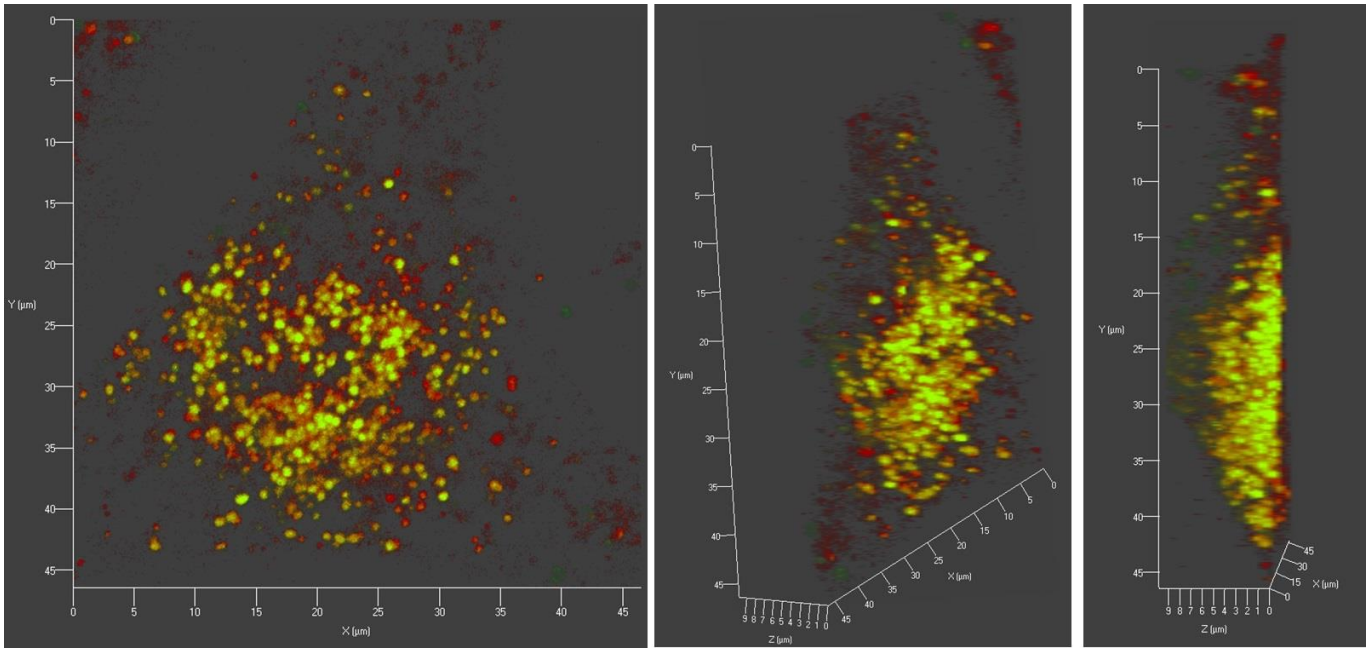

Figure S23. Representative image showing the maximum intensity projection of *Z* sections with the vertical slice representing the *yz*-axis and the horizontal slice representing the *xz*-axis. HeLa cells were incubated with the NPs formed from **3** (4 μM) for 4 h. The red fluorescence arose from Lyso Tracker Red, the green fluorescence arose from **3**, and the yellow fluorescence was the merge of red and green channels.

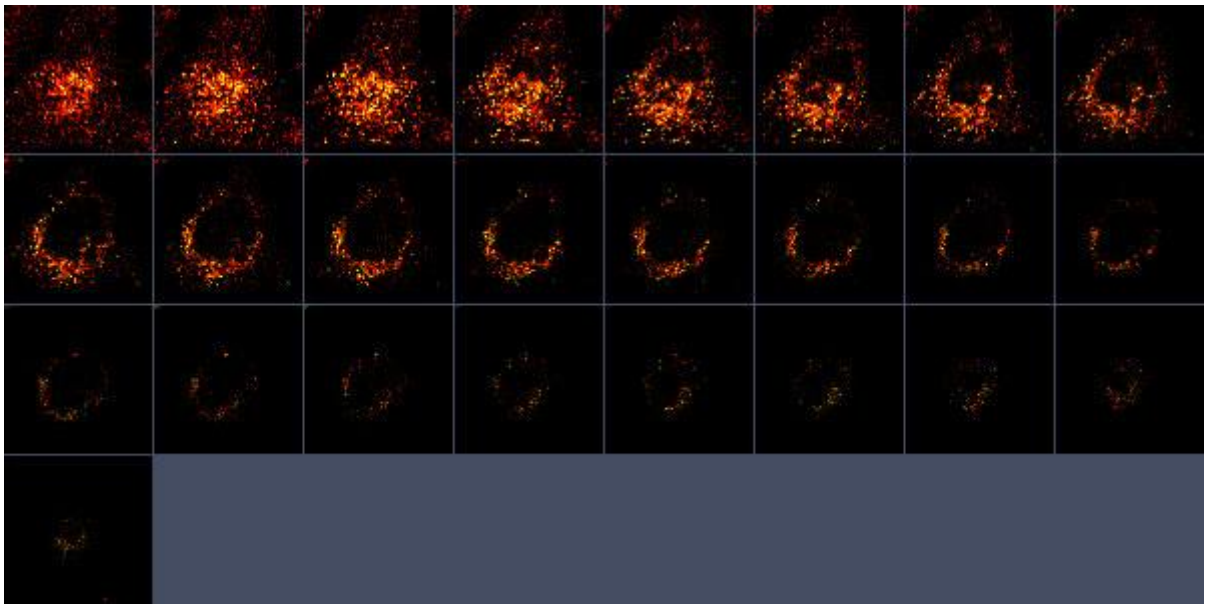

Figure S24. *Z*-stack confocal laser scanning microscopy images of HeLa cell line after 4 h incubation with the NPs formed from **3**.

From Figures S22–S24, well overlap between green fluorescence arising from **3** and red fluorescence arising from Lyso Tracker Red was observed, demonstrating that the cells uptook the NPs formed from **3** *via* endocytosis.

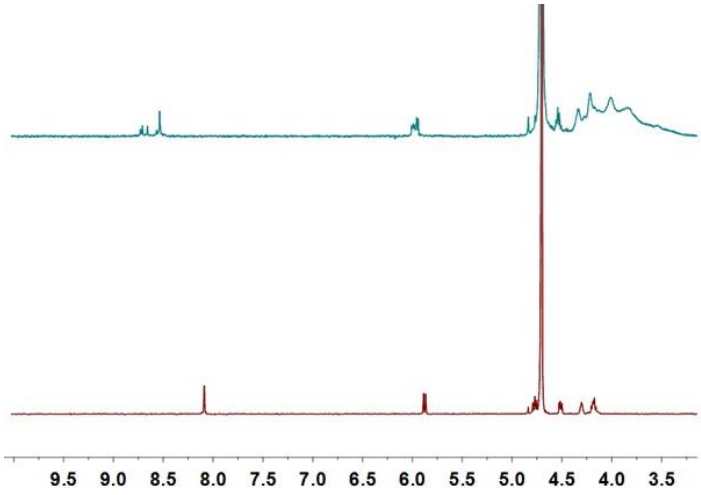

Figure S25. Partial ^{1}H NMR spectra (500 MHz, D_2O, 293K): (top) GTP (2.00 mM) in the presence of **2** (2.00 mM); (bottom) GTP (2.00 mM).

Chemical shift changes on GTP were monitored in the presence **2**, confirming the coordination between the N_7 atoms of purine bases on DNA and the Pt centers (*SI Appendix*, Fig. S25).

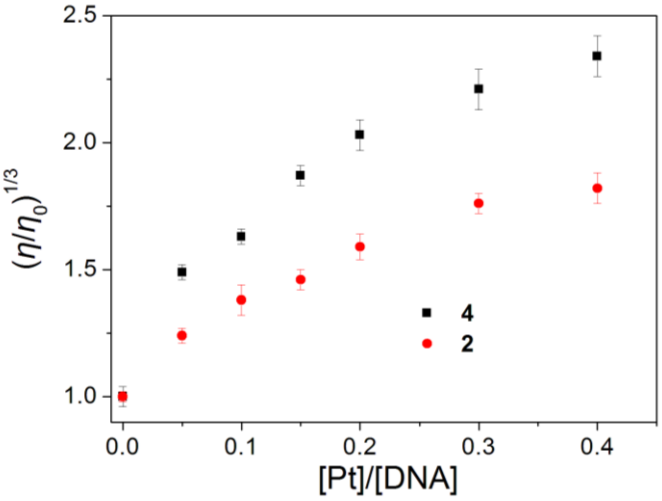

Figure S26. Change in relative viscosity of ctDNA (200 μM) on increasing the concentration of **2** and **4**.

The average flow times of each sample (t) [corrected by average flow time of buffer alone (t_0) and recorded in triplicate] were calculated using Schott AVS 310 automated viscometer. The relative viscosities (η) were obtained from the average flow time values using the equation: $\eta = (t - t_0)/t_0$. The data was presented as a plot of relative specific viscosity $[(\eta/\eta_0)^{1/3}]$ *vs*. [Pt]/ [DNA], where η and η_0 are the viscosities of ctDNA in the presence and absence of **2** (or **4**).

Viscometry experiments showed a gradual enhancement in the relative viscosity (η/η_0) of a solution containing calf-thymus DNA (ctDNA) as the concentration of **4** was increased, and the increase in η/η_0 was much lower for the ctDNA solution treated with **2** at the same concentration of Pt (*SI Appendix*, Fig. S26). These results indicate that the metallacage delivers Pt(II) in a more relevant form for interactions with DNA versus the triflate precursor.

2. Cytotoxicity evaluation

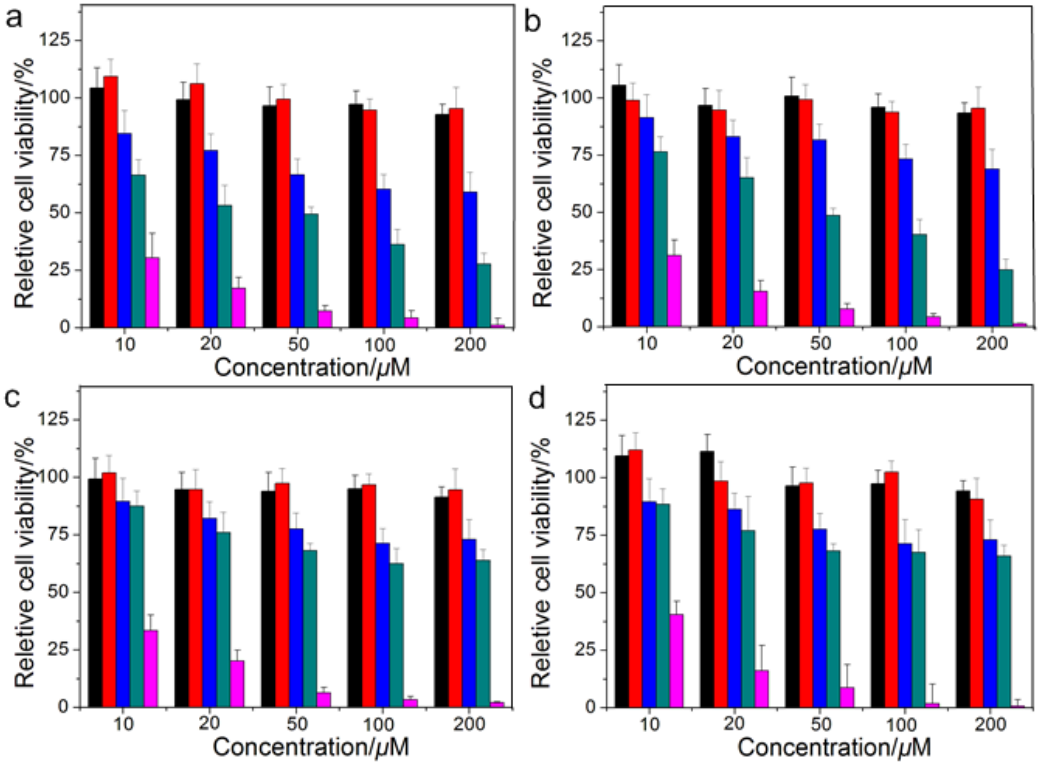

Figure S27. Cytotoxicity of **1** (black column), **3** (red column), **MNPs** pre-treated with free biotin (blue column), **MNPs** (green column) and **2** (pink column) against (a) HeLa, (b) HepG2, (c) HEK293 and (d) CHO cells with the concentrations ranging from 10 to 200 μM.

*3. Cellular uptake of the **MNPs** determined by ICP-MS*

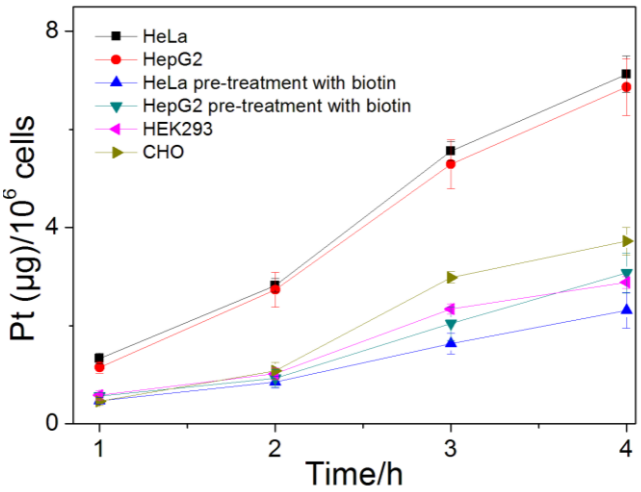

Figure S28. Quantitative analysis of the platinum amount in HeLa, HepG2, CHO and HEK293 cells after incubation with the **MNPs** for 1 h, 2 h, 3 h, and 4 h, respectively.

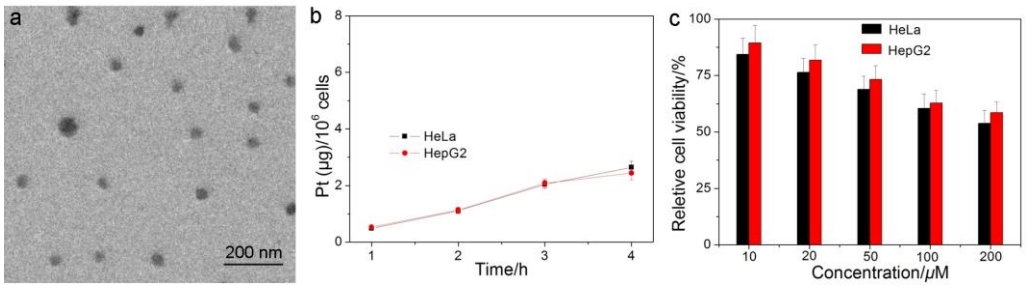

Figure S29. (a) TEM image of the metallacage-loaded nanoparticles fabricated from **mPEG-DSPE** without biotin groups. (b) Quantitative analysis of the platinum amount in HeLa and HepG2 cells after incubation with the metallacage-loaded nanoparticles fabricated from **mPEG-DSPE** for 1 h, 2 h, 3 h, and 4 h, respectively. (c) Cytotoxicity of the metallacage-loaded nanoparticles fabricated from **mPEG-DSPE** against HeLa and HepG2 cells with the concentrations ranging from 10 to 200 μM.

Table S1. Platinum content per milligram of protein in the nucleus and cytoplasm (ng Pt/mg protein) of different cell lines after treatment for 6 h with **MNPs** (the concentration of Pt was 10.0 μM) following an established procedure.[S4]

HeLa		HepG2		CHO		HEK293	
nucleus	cytoplasm	nucleus	cytoplasm	nucleus	cytoplasm	nucleus	cytoplasm
128 ±23.4	1.76 ±0.210	115 ±18.4	1.54 ±0.182	46.3 ±5.47	0.582 ±0.110	40.3 ±4.25	0.461 ±0. 091

To have a more complete understanding of the cellular response induced by **MNPs**, we evaluated their mode of cell killing. Apoptosis is the process of programmed cell death. Annexin V-FITC together with propidium iodide (PI) has been widely used as fluorescent probe to distinguish viable cells from dead cells of different stages, namely, viable (AnnexinV-FITC−/PI−), early apoptotic (Annexin V-FITC+/PI−), late-stage apoptotic (Annexin V-FITC+/PI+) and necrotic (Annexin V-FITC−/PI+) cells, because FITC can bind to the membrane of apoptotic cells that express phosphatidylserine, while PI can penetrate into the necrotic cells to stain the nucleus. On the other hand, in order to eliminate the influence of the fluorescence arising from the metallacage that is similar to that of FITC, we chose **2** as the model compound to further determine the percentage of apoptotic cells after exposure to **2** in HeLa and HepG2 cells using flow cytometry. As shown in Table S2, **2** induced large populations of HeLa (16.7% for early apoptosis; 10.0% for later apoptosis; 2.40% for necrosis) and HepG2 cells (14.8% for early apoptosis; 9.19% for later apoptosis; 2.33% for necrosis) to undergo early- and late-stage apoptosis.

Table S2. Apoptosis induced against HeLa and HepG2 cells by **2** after 24 h incubation using an annexin-V FITC/PI assay.

	live cells	early apoptotic cells	late apoptotic cells	necrotic/dead cells
HeLa	70.9%	16.7%	2.40%	10.0%
HepG2	73.7%	14.8%	2.33%	9.19%

4. In vivo studies

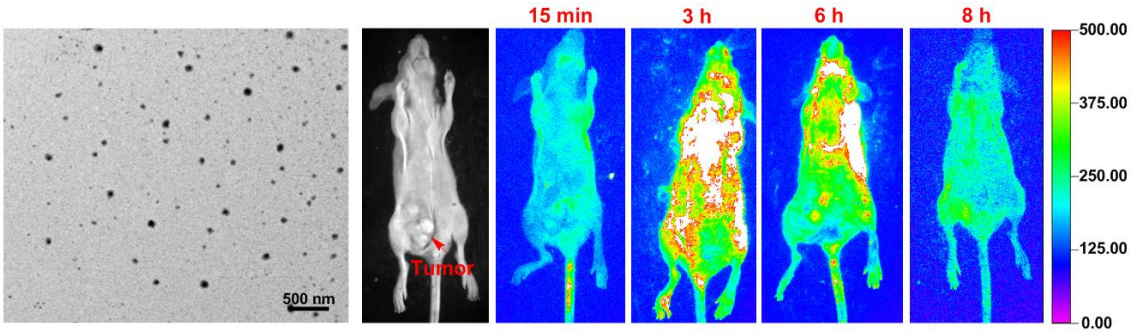

Figure S30. (Left) Nanoparticles fabricated from **3** through a reprecipitation technique.[S5] (Right) Representative fluorescence imaging of nude mice bearing HeLa cancer xenograft following *i.v*. injection of the nanoparticles fabricated from **3**.

Although the size of the NPs formed from **3** was similar to that of the **MNPs**, the fluorescence signal in the body annihilated much faster and no targeting phenomenon was observed for the mice after administration of the NPs fabricated from **3**. The reason was that the NPs fabricated from **3** without PEG shell were easily uptaken by the immune system, such as the reticuloendothelial system located in the reticular connective tissue. On the other hand, the NPs without targeting groups decrease their accumulation in the tumor tissue. These phenomenon confirmed longer blood circulation of the PEGylated **MNPs** and targeting delivery to tumor tissue through EPR effect after *i.v* injection.

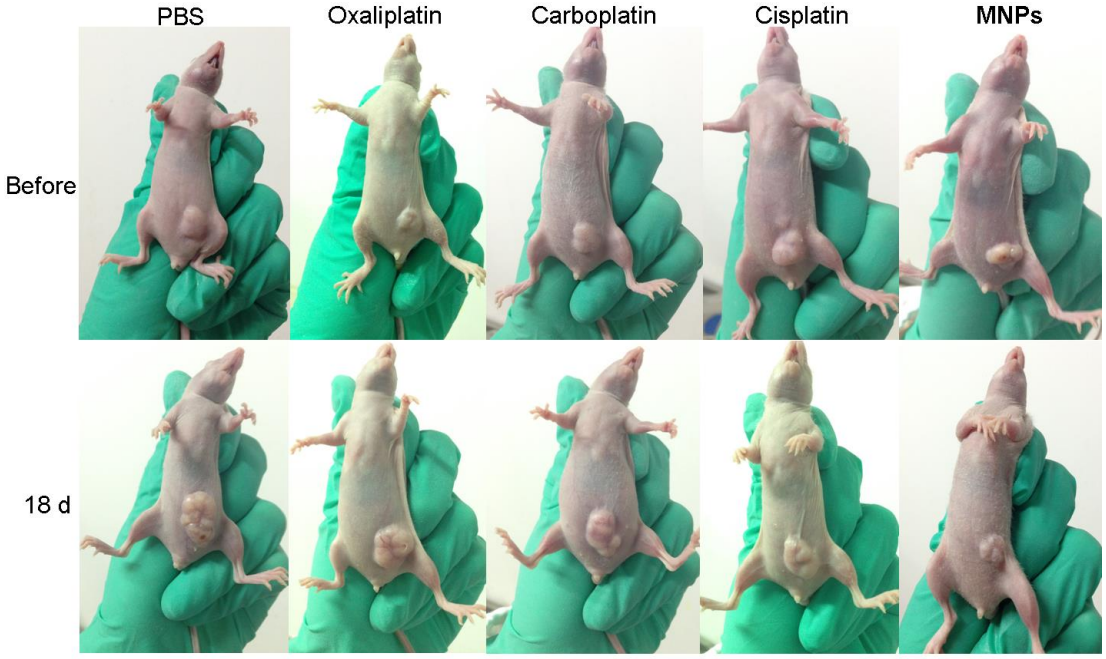

Figure S31. Representative photos of mice bearing HeLa tumor before and after administration of PBS, oxaliplatin, carboplatin, cisplatin or **MNPs**.

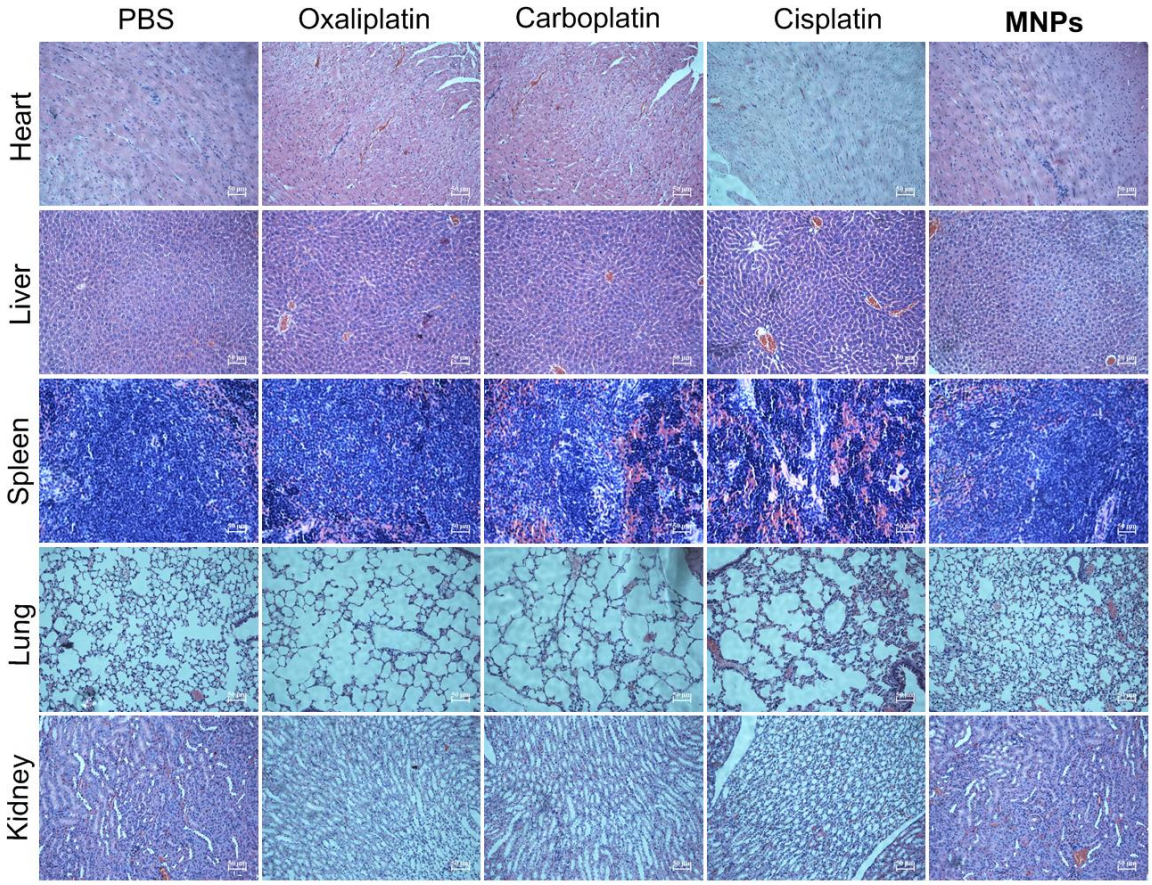

Figure S32. H&E stained images of heart, liver, spleen, lung and kidney from different groups after intravenous injection of PBS, oxaliplatin, carboplatin and cisplatin or **MNPs**.

As shown in Figure S32, histological analyses of the major organ slices of the mice treated with **MNPs** exhibited no obvious tissue damage. However, in terms of oxaliplatin- or carboplatin-treated groups, especially for the cisplatin-treated group, notable nephrotoxicity, pulmonary and hepatic damage were observed. The systemic toxicity of the **MNPs** was effectively reduced, arising from greatly reduced delivery of Pt(II) to normal tissue compared to tumor sites. These data confirmed that our newly developed theranostic nanomaterial exhibited the improved efficacy for cancer therapy with lower systemic toxicity, compared with the free anticancer drugs.

Section D. References

S1 Duan XF, et al. (2006) Insights into the general and efficient cross McMurry reactions between ketones. *J. Org. Chem*. 71: 9873–9876.

S2 Wang M, et al. (2010) Metallosupramolecular tetragonal prisms via multicomponent coordination-driven template-free self-assembly. *J. Am. Chem. Soc*. 132: 6282–6283.

S3 Zhu Z, Swager TM (2001) Conjugated polymers containing 2,3-dialkoxybenzene and iptycene building blocks. *Org. Lett*. 3: 3471–3474.

S4 Naik A, et al. (2014) Visible-light-induced annihilation of tumor cells with platinum-porphyrin conjugates.

Angew. Chem. Int. Ed. 53: 6938–6941.

S5 Jana A, et al. (2012) Perylene-3-ylmethanol: fluorescent organic nanoparticles as a single-component photoresponsive nanocarrier with real-time monitoring of anticancer drug release. *J. Am. Chem. Soc*. 134: 7656–7659.

S6 Yan X, Cook TR, Wang P, Huang F, Stang PJ (2015) Highly emissive platinum(II) metallacages. *Nature Chem.* 7: 342–348.

S7 Naik A, Rubbiani R, Gasser G, Spingler B (2014) Visible-light-induced annihilation of tumor cells with platinum-porphyrin conjugates. *Angew. Chem. Int. Ed.* 53: 6938–6941.